CHEMISTRY OF MATERIALS

Methods/Protocols

pubs.acs.org/cm

Measuring the Glass Transition Temperature of Conjugated Polymer Films with Ultraviolet−Visible Spectroscopy

Samuel E. Root,[‡] Mohammad A. Alkhadra,[‡] Daniel Rodriquez, Adam D. Printz, and Darren J. Lipomi*

Department of NanoEngineering, University of California, San Diego, 9500 Gilman Drive, Mail Code 0448, La Jolla, California 92093-0448, United States

Supporting Information

ABSTRACT: The glass transition temperature (T_g) of a conjugated polymer can be used to predict its morphological stability and mechanical properties. Despite the importance of this parameter in applications from organic solar cells to wearable electronics, it is not easy to measure. The T_g is often too weak to detect using conventional differential scanning calorimetry (DSC). Alternative methods—e.g., variable temperature ellipsometry—require specialized equipment. This paper describes a technique for measuring the T_g of thin films of semicrystalline conjugated polymers using only a hot plate and an ultraviolet−visible (UV−vis) spectrometer. UV−vis spectroscopy is used to measure changes in the absorption spectrum due to molecular-scale rearrangement of polymers when heated past T_g, corresponding to the onset of the formation of photophysical aggregates. A deviation metric, defined as the sum of the squared deviation in absorbance between as-cast and annealed films, is used to quantify shifts in the absorption spectra. The glass transition is observed as a change in slope in a plot of the deviation metric versus temperature. To demonstrate the usefulness of this technique, a variety of semiconducting polymers are tested: P3BT, PBTTT-C14, F8BT, PDTSTPD, PTB7, PCDTBT, TQ1, and MEH-PPV. These polymers represent a range of solid-state morphologies, from highly ordered to predominantly amorphous. A successful measurement of T_g depends on the ability of the polymer to form photophysical aggregates. The results obtained using this method for P3BT, PBTTT-C14, F8BT, and PDTSTPD are in agreement with values of T_g that have been reported in the literature. Molecular dynamics simulations are used to show how the morphology evolves upon annealing: above the T_g, an initially kinetically trapped morphology undergoes structural rearrangement to assume a more thermodynamically preferred structure. The temperature at which onset of this rearrangement occurs in the simulation is concomitant with the spectroscopically determined value of T_g.

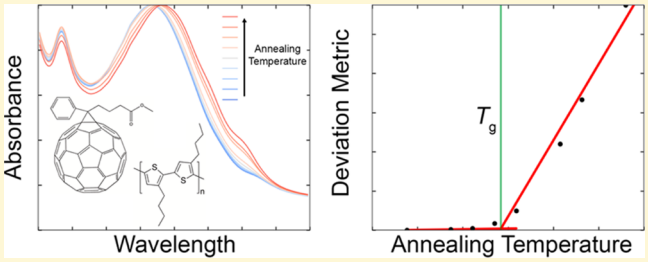

INTRODUCTION

The glass transition temperature (T_g) is a critical property of polymers that can be used to predict the thermal[1] and mechanical stabilities[2] of organic semiconductor devices.[3] The glass transition describes the onset of relaxation processes in segments of the main chains of polymeric materials.[4−6] This parameter is of particular importance for the operational stability of organic electronic devices (which include π-conjugated polymers and small molecules) for at least two reasons.[1] First, devices operating above T_g may undergo deleterious morphological rearrangements. Changes in the morphology are deleterious particularly if a kinetically trapped structure formed upon solidification of a film is conducive to device performance, while a thermodynamically favorable structure that forms when heated is not. For example, the domains in a highly phase-separated morphology of a bulk heterojunction (BHJ) organic solar cell that forms upon heating above T_g may be too large to allow efficient separation of charges.[1] Second, the T_g is intimately related to stress-relaxation processes of polymeric materials. For soft, compliant polymers intended for biological integration, it may be desirable to have a low T_g, and thus rubber-like mechanical behavior.[7,8]

Although a variety of well-developed methods exist for measuring the T_g of bulk polymeric materials,[9] thin films present a significant challenge for these conventional methods. The challenge arises in part because of the small thermal signal produced by the minute mass of a thin film. Moreover, the thermal properties of the bulk material do not necessarily represent those of a thin film.[10] This paper describes a facile technique to measure the T_g's of conjugated polymers that leverages their unique photophysical behavior. The technique works by finding the annealing temperature at which the thin-film absorption spectrum in the UV−vis range undergoes an abrupt change, indicating the onset of formation of photophysical aggregates.[11]

Thin films of conjugated polymers are generally prepared by casting from a solution using laboratory-scale techniques (e.g., spin coating) or industrial-scale techniques (e.g., slot-die coating, gravure, inkjet, or screen printing). Rapid solidification of the polymer that occurs upon evaporation of the solvent

Received: January 18, 2017
Revised: March 10, 2017
Published: March 14, 2017

DOI: 10.1021/acs.chemmater.7b00242
Chem. Mater. 2017, 29, 2646−2654

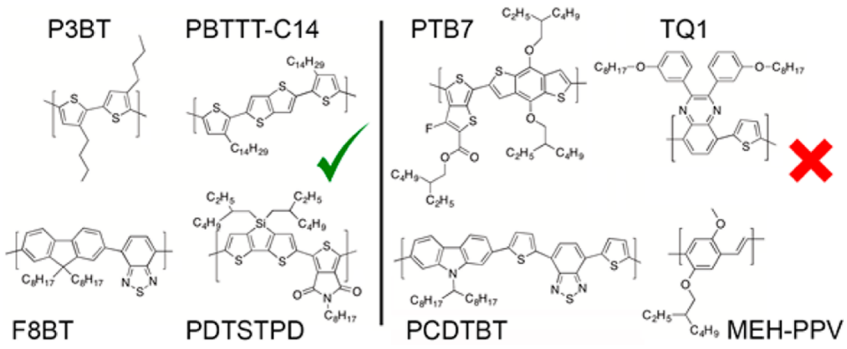

Figure 1. Chemical structures and common names of conjugated polymers involved in this study. Refer to Experimental Methods for systematic names. The technique works best for semicrystalline polymers.

typically results in the formation of kinetically trapped structures that contain considerable free volume[12] and structural disorder.[13] Thermal annealing is a common postprocessing step that allows kinetically trapped structures to undergo morphological rearrangement and aggregation.[14] These structural changes have important effects on device-scale optoelectronic[15] and mechanical properties.[2]

In a recent review on the glass transition of organic semiconductors,[1] four standard techniques to measure T_g were outlined: differential scanning calorimetry (DSC),[18] dynamic mechanical analysis (DMA),[17] broadband dielectric spectroscopy (BDS),[18] and variable-temperature ellipsometry (VTE).[19] These techniques are ubiquitous in the field of polymer science and have been widely applied to characterize the thermal properties of semiconducting polymers, for which the most common is DSC.[16] In many cases, DSC does not possess the sensitivity to detect the subtle glass transitions of polymeric semiconductors; it is commonplace for T_g to evade detection, even in cases where DSC thermograms are reported.[15,20−26] Moreover, conventional DSC setups require bulk samples and thus cannot be used to characterize thin films (DMA and BDS are also typically restricted to bulk materials).[1] Advanced techniques such as differential AC-chip calorimetry have been developed to mitigate some of these limitations,[27] however, they are usually unavailable in laboratories that focus on organic electronics.

The thermal behavior of a polymeric thin film becomes thickness-dependent below a critical threshold (~100 nm).[28] This phenomenon has been attributed to interfacial effects at the free surface and with the supporting substrate.[19,28] The dominant effect is the increased mobility of polymer chains at the free surface, which serves to decrease the T_g.[19] VTE is unique among the available thermal characterization techniques in that it can probe thermal transitions of thin films, as opposed to bulk samples.[19] Unfortunately, ellipsometric systems, especially those with temperature-controlled stages, are expensive and not widely available. Therefore, use of this technique is mainly restricted to research groups that have specialized expertise.

Thin films of conjugated polymers absorb strongly in the UV−vis range, and various optical techniques have been developed to characterize their thermomechanical properties.[20,29,30] Lindqvist et al. have developed a simple technique to measure thermal transitions in fullerene-based BHJ films by taking advantage of the increased scattering of micrometer-sized fullerene crystals that form when the film is annealed above the T_g.[20] As such, this technique is not applicable to neat conjugated polymer films.

In this work, we measured the T_g by taking advantage of the shift in the UV−vis absorption spectrum that occurs after thermally annealing many neat conjugated polymer films.[11,31] This shift has been widely attributed to the formation of ordered aggregates and is generally accompanied by an improvement in the charge transport properties of the thin film.[11] The amorphous phase of conjugated polymer thin films undergoes significant structural rearrangement only when the annealing temperature approaches T_g. We thus hypothesized that it would be possible to estimate the T_g of conjugated polymer thin films by quantifying the change in the absorption spectrum that resulted from thermal annealing. We expected that, once the annealing temperature surpassed the T_g, there would be an easily discernible change in the absorption spectrum. Hence, we defined a deviation metric (DM_T) as the sum of the squared deviation in the absorbance between as-cast and annealed films (at annealing temperature, T):

$$DM_T \equiv \sum_{\lambda_{min}}^{\lambda_{max}} [I_{RT}(\lambda) - I_T(\lambda)]^2 \quad (1)$$

where $I_{RT}(\lambda)$ and $I_T(\lambda)$ are the normalized absorption intensities of the as-cast (room temperature) and annealed films, respectively, λ is the wavelength, and λ_{min} and λ_{max} are the lower and upper bounds of the optical sweep, respectively. We expected that, at the T_g, there would be a sharp increase in the slope of DM_T when plotted against annealing temperature.

EXPERIMENTAL DESIGN

Selection of Materials. To test the validity of our proposed methodology, we selected materials whose T_g's had been measured successfully using other techniques. Moreover, it was important to use materials of significant interest to the research community. Since the T_g of the popular regioregular poly(3-hexylthiophene) (P3HT) is near or somewhat below room temperature, we selected poly(3-butylthiophene) (P3BT) instead (structure shown in Figure 1). An additional advantage of using P3BT was that we were able to apply the weakly interacting H-aggregate model developed by Spano and co-workers to provide a detailed analysis of vibronic progression as a function of annealing temperature for polythiophenes.[32,33] This analysis allowed us to deconvolute spectral shifts and determine microstructural mechanisms responsible for the abrupt shift in the absorption spectrum near the T_g. Additionally, to demonstrate the applicability of our technique to composite systems of organic semiconductors, we tested a

DOI: 10.1021/acs.chemmater.7b00242
Chem. Mater. 2017, 29, 2646−2654

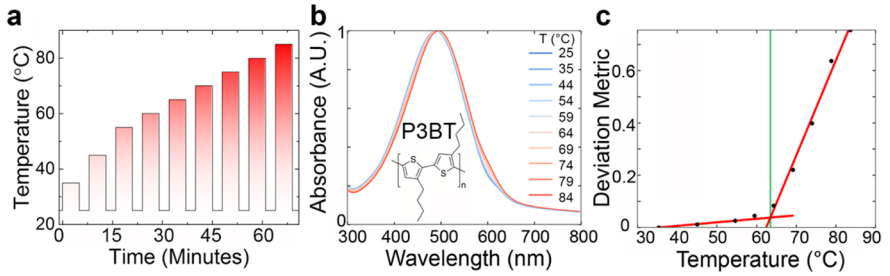

Figure 2. Overview of UV−vis absorption T_g measurement technique for P3BT. (a) Thermal history of polymer thin film. Absorption measurements were taken at ambient temperature for the as-cast film and between successive annealing steps. (b) Thin-film absorption spectra for the annealing temperatures indicated. (c) Evolution of the deviation metric as a function of annealing temperature, showing a distinct increase at the T_g of P3BT.

BHJ film comprising P3BT and [6,6]-phenyl C_{61} butyric acid methyl ester (PCBM).

To assess the transferability of our proposed methodology, we performed the experiment on several conjugated polymers with complex structures. The following materials were tested: F8BT, PBTTT-C14, PDTSTPD, PTB7, PCDTBT, TQ1, and MEH-PPV. These materials were chosen because they exhibit a wide range of ordering in the solid state, from highly ordered (e.g., the liquid-crystalline PBTTT-C14) to minimal long-range order (e.g., TQ1). In particular, PDTSTPD was chosen because its T_g has been reported,[34,35] and we have previously performed molecular dynamics (MD) simulations to predict its thermal and mechanical properties.[36] To gain a detailed mechanistic understanding of our results, we performed additional MD simulations to demonstrate how the thermal annealing of a kinetically trapped structure results in morphological rearrangement. We expected that materials with stronger tendencies to crystallize would produce shifts in the absorption spectra that were more pronounced, corresponding to a more easily observable T_g. Accordingly, we did not expect this technique to work for predominantly amorphous materials (refer to Section 1 of the Supporting Information). These amorphous materials are generally blended with fullerenes to form BHJs and do not perform especially well in transistor devices. Thus, the properties of the neat polymers are not as relevant as those of the BHJ, and the optical technique of Lindqvist et al. (which relies on the presence of the fullerene) can be applied instead.[20]

Design of Annealing Protocol. The experimental protocol was specifically designed so that it would only require basic equipment readily available to any research group interested in conjugated polymers: a spin coater, a hot plate, a glovebox, and a UV−vis spectrometer. All thermal annealing was carried out inside a glovebox (N_2 atmosphere) to eliminate possible effects of photochemical degradation at elevated temperatures that could occur under ambient conditions. For example, Cho et al. observed a significant degradation in the $\pi-\pi^*$ absorption band of PCDTBT when annealed above the T_g in air.[37] Thermal annealing was carried out using a standard hot plate, and heat transfer calculations were performed to account for thermal insulation by the glass slide substrate, as described in detail in Section 2 of the Supporting Information. The UV−vis characterization was performed ex situ because a UV−vis spectrometer with a controlled atmosphere and temperature-controlled stage is not a common piece of equipment. This is not to say that in situ measurements are not viable, as Pingel et al. studied the thermal dependence of UV−vis absorption in situ for deuterated P3HT.[33] However, no evidence of the glass transition was observed in those experiments because the T_g of P3HT is below room temperature. For our experiments, each film was subjected to a thermal cycling protocol, like the one shown in Figure 2a. UV−vis spectra of the cooled films under ambient conditions were taken between annealing steps. To analyze the data and extract the T_g, we developed a code to automate and standardize the bilinear regression analysis based on a custom R^2 maximization algorithm (we released this algorithm in an open-sourced format; refer to Section 3 of the Supporting Information).

RESULTS AND DISCUSSION

Proof-of-Concept: P3BT. The results of our proposed technique—as applied to P3BT—are shown in Figure 2. The thermal cycling protocol is given in Figure 2a. After each annealing step, a UV−vis spectrum was recorded (Figure 2b). We observed that the spectra exhibited a clear redshift as well as a distinct change in shape around 600 nm with increased annealing temperature. These shifts in the absorption spectra result from the formation of weakly interacting H-aggregates, as explained in the next section. Spectra were processed using the deviation metric, and this quantity was plotted against annealing temperature (Figure 2c); a clear transition was observed. Using our bilinear curve-fitting algorithm, the T_g was estimated to be 60 ± 3 °C. Encouragingly, this measurement was in excellent quantitative agreement with reported values in the literature, which range from 59 to 67 °C.[38,39]

Weakly Interacting H-Aggregate Analysis. To identify the microstructural changes responsible for the evolution of the absorption spectra upon annealing, we applied the weakly interacting H-aggregate model, developed by Spano and coworkers.[32,40] When two segments of planar thiophene backbones come into cofacial contact, an excitonic coupling produces a redshift in the absorption. This spectral signature is known as an H-aggregate,[41] and the absorption spectra of poly(3-alkylthiophenes) can be comprehensively analyzed using this model.[32] To perform this analysis, a Franck−Condon progression was fit to the UV−vis spectra (assuming a Gaussian line shape), and the absorption of the aggregated regions was deconvoluted from that of the amorphous phase. A representative fit obtained from this process is shown in Figure 3a. After correcting for the unequal absorption coefficients of the two domains, the fraction of aggregated polymeric chromophores was determined.

As shown in Figure 3b, we found that the aggregate fraction increased with annealing temperature and exhibited a transition near the T_g. Interestingly, we observed not only a change in the slope but also an increase in the error (based on the standard deviation between independently tested films). It is possible that the increase in the statistical uncertainty is due to minor

DOI: 10.1021/acs.chemmater.7b00242
Chem. Mater. 2017, 29, 2646−2654

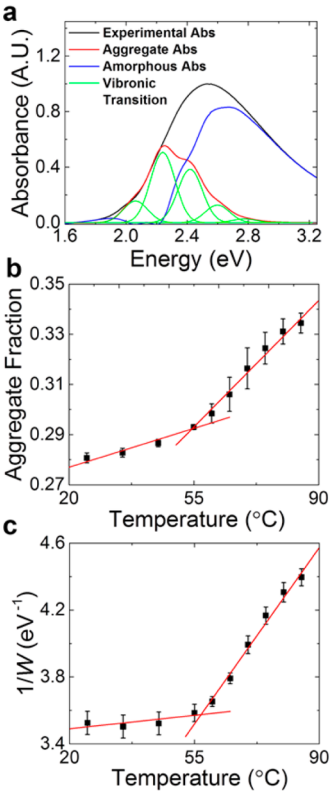

Figure 3. Weakly interacting H-aggregate analysis of P3BT. (a) Representative deconstructed absorption spectrum used to calculate (b) the aggregate fraction and (c) the inverse exciton bandwidth, $1/W$.

differences in the cooling rates of separately annealed films. The H-aggregate model can also be used to characterize the quality of structural ordering present in aggregate regions.

The free exciton bandwidth (W) is the dispersion of energy that arises due to interchain coupling in the aggregate domains. This parameter is inversely related to the conjugation length of the interacting chromophoric species.[32,42] As shown in Figure 3c, the inverse exciton bandwidth $1/W$ exhibits a sharp transition when the film is annealed above the T_g. This observation is in agreement with previous results of Yazawa et al., who used temperature-dependent Fourier-transform infrared absorption measurements to correlate the glass transition in P3BT with the thermal activation of the dihedral twist between two thiophene rings.[39] We also found that the $1/W$ exhibited a sharper transition than the aggregate fraction.

Bulk Heterojunction Film. Conjugated polymers are typically blended with solubilized fullerene derivatives to form the active layer of BHJ organic photovoltaic devices. The thermal behavior of such composites is important for both optimization of device processing and operational stability.[1] Fullerenes are known to slow the dynamics of conjugated polymers.[43] Due to the strong dispersive forces and spherical geometries, fullerenes act as antiplasticizers and increase the T_g of the composite.[2,44] To demonstrate the applicability of our approach for such composites, we have characterized a BHJ layer composed of P3BT and PCBM. The results of our technique are shown in Figure 4. As expected, we found that the addition of PCBM served to increase the T_g by about 15 °C. Moreover, we found that the addition of 1,8-diiodooctane, a common processing additive, resulted in a significant decrease in the T_g of the BHJ film (Supporting Information, Section 4).

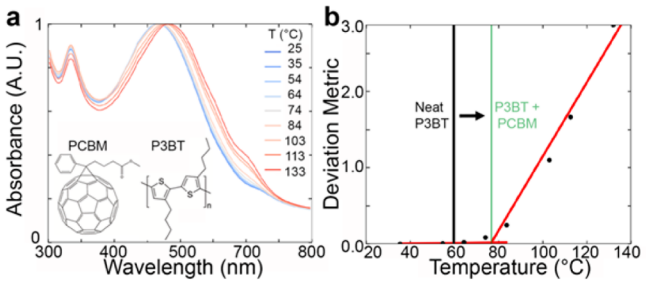

Figure 4. Thermal characterization of a BHJ film P3BT:PCBM (0.8:1 by mass). (a) UV−vis absorption spectra for different annealing temperatures. (b) Deviation metric showing a distinct transition at 75 °C. The addition of PCBM resulted in a ∼15 °C shift in the T_g.

PBTTT-C14. The PBTTT family of polymers are known to exhibit a highly ordered, liquid-crystalline mesophase. As shown in Figure 5a, our technique revealed a distinct transition occurring at 102 ± 1 °C for PBTTT-C14. Previous DSC measurements have revealed two discrete exotherms upon cooling. These two transitions occur at ∼100 °C and ∼230 °C and have been rigorously assigned to the crystallization of the side chains and the backbone, respectively.[45−47] However, the DSC thermograms reported for PBTTT-C14 revealed no indication of a glass transition. We have rationalized this finding through the argument that the weak signal of the glass transition could be obscured by the endothermic melting of the side chains, as both occur in the same temperature range. This argument is further substantiated by the temperature-dependent UV−vis spectroscopic ellipsometry measurements of DeLongchamp et al., which revealed that the thermochromic behavior of PBTTT-C14 remains approximately constant until heated to ∼120 °C.[46] These results suggest that segmental relaxation of the conjugated backbone can be intrinsically coupled to the dynamics of the side chains, which could lead to convoluted signals in DSC thermograms.

F8BT. The polyfluorene copolymer, F8BT, has been of particular interest for photovoltaic applications due to its ability to act as the electron acceptor in BHJ devices.[48] As shown in Figure 5b, our technique revealed a pronounced transition at 104 ± 6 °C. F8BT has been previously characterized with both DSC and VTE. DSC measurements revealed an exothermic feature at 125 °C, which Sirringhaus and co-workers assigned to the glass transition; an additional, more pronounced exothermic transition at 240 °C has been assigned to the crystallization temperature.[49] The authors argued that cold crystallization might also be occurring at the T_g as the chains become mobile. Additionally, VTE experiments revealed a sharp transition in the ellipsometric angle at ∼100 °C.[50] The slight negative deviation in our measurement from the DSC measurements was likely due to thin-film effects, since our measurement agreed with the transition in the ellipsometric angle obtained with thin films using VTE.

PDTSTPD. The donor−acceptor polymer PDTSTPD is a commercially available conjugated polymer that exhibits a high photovoltaic conversion efficiency when blended with fullerenes and incorporated into a BHJ device.[34,35,51] The T_g has been reported to be 109 °C based on DSC measurements.[34] In close agreement with these results, we have measured the T_g to be 106 ± 12 °C (Figure 5c). We note that the transition was not quite as pronounced as it was for the other polymers tested, leading to substantially more uncertainty in the measured value. We ascribed this finding to two factors: a small overall change

DOI: 10.1021/acs.chemmater.7b00242
Chem. Mater. 2017, 29, 2646−2654

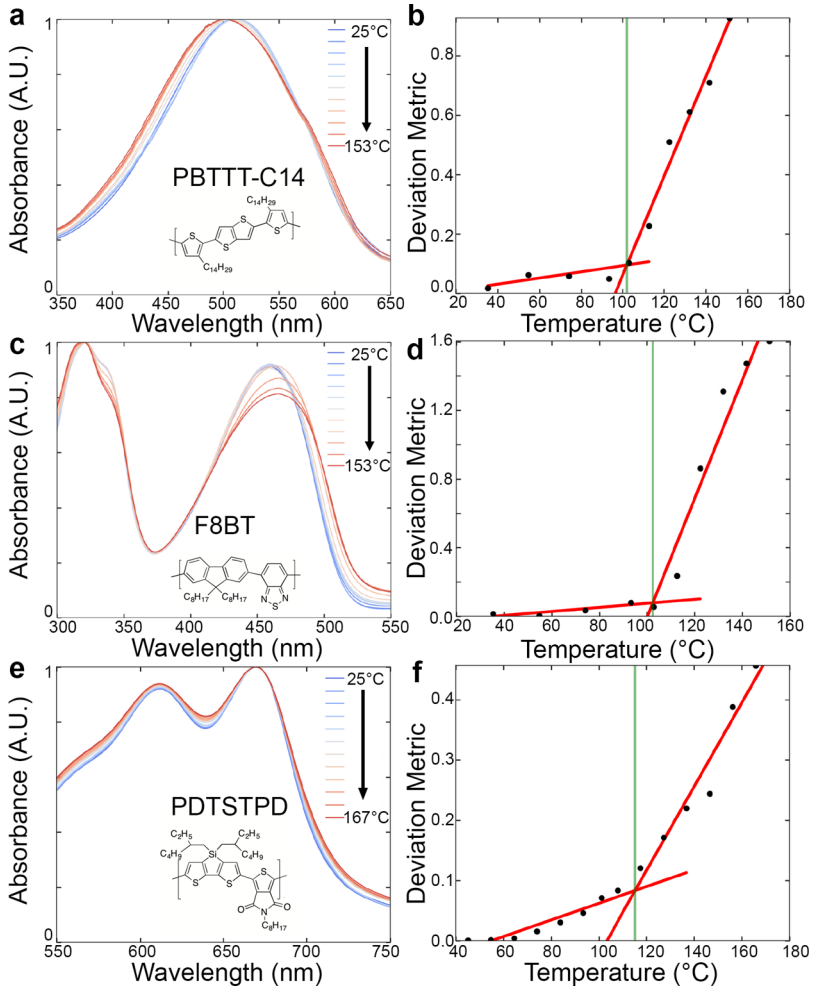

Figure 5. Application of technique to representative semiconducting polymers. UV−vis absorption spectra and corresponding deviation metric showing the measurement of the T_g for (a) PBTTT-C14, (b) F8BT, and (c) PDTSTPD.

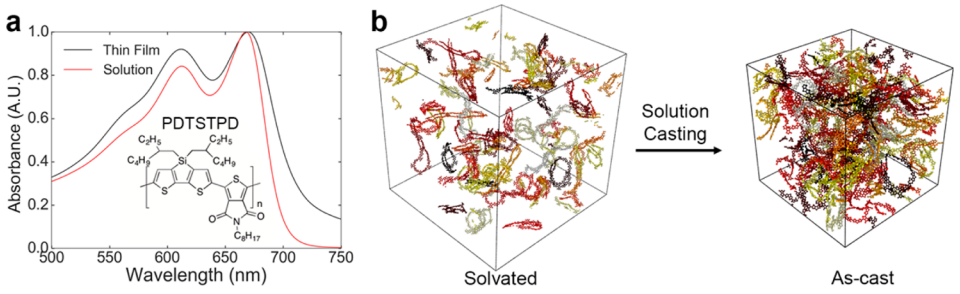

Figure 6. Simulated solution casting: experimental justification and MD snapshots. (a) Comparison between thin-film and solution-phase absorption spectra showing aggregate behavior in a dilute solution. (b) Snapshots showing the trajectory of the simulated solution casting; individual molecules are colored separately, and side chains are not shown.

in the absorption spectrum with annealing and the occurrence of morphological rearrangement during sub-T_g annealing of this material.[52] When the best fits are not entirely obvious, the fitting algorithm described in Section 3 of the Supporting Information is especially important for the accurate determination of the T_g.

Molecular dynamics simulations have previously predicted a value of 107 ± 10 °C for the T_g of PDTSTPD.[53] This prediction was achieved by subjecting an initially melted polymeric simulation to a thermal quenching protocol at constant pressure. The density was monitored as a function of temperature, and the glass transition was taken as the intersection of linear fits to the melted and glassy regions. The thermal history in our proposed measurement technique is fundamentally different: an initially kinetically trapped morphology is gradually heated until polymeric motion becomes activated and chain segments can relax to a state closer to thermodynamic equilibrium. To obtain an improved understanding of this process, we performed additional simulations that provide a closer representation of the experimental protocol.

DOI: 10.1021/acs.chemmater.7b00242
Chem. Mater. 2017, 29, 2646−2654

First, we generated a simulated morphology to represent an as-cast film that was kinetically trapped at room temperature. The procedure for simulating solution casting was guided by solution-phase UV−vis absorption measurements and previous work.[54] As shown in Figure 6a, the UV−vis absorption spectra of a dilute solution (0.015 mg mL^{-1}, chloroform) and an as-cast thin film of PDTSTPD both contain aggregate absorption peaks. Fauvell et al. recently demonstrated that this low-energy visible absorption is due to self-aggregation-induced ordering (rather than in-chain charge transfer, as previously thought).[54] Thus, to generate the as-cast morphology, self-aggregated chains were randomly packed at low concentration and allowed to condense at room temperature and atmospheric pressure until the density stabilized (Figure 6b). A detailed description of this process and the results of such simulations can be found in an earlier publication.[36] It has been previously demonstrated that simulation morphologies generated in this manner give a closer match to the experimentally determined tensile modulus of an as-cast film.

The morphology generated by solution casting was far from thermodynamic equilibrium and contained significant void space and disorder, as shown in Figure 7(1). The system was

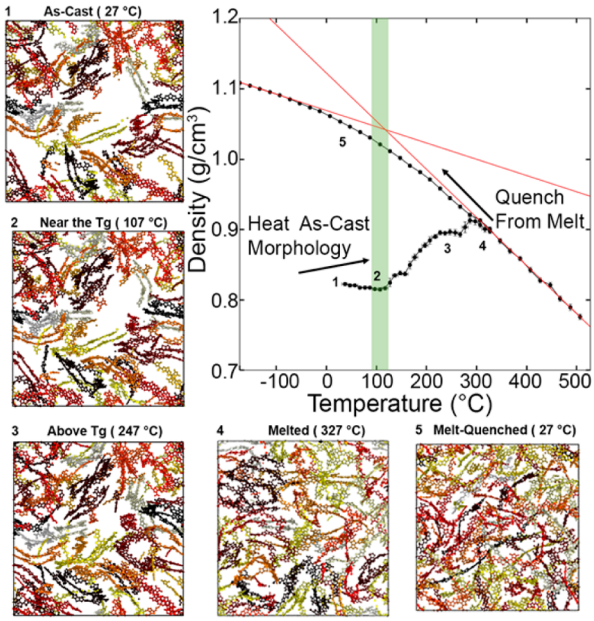

Figure 7. MD simulations showing the thermally activated molecular and microstructural rearrangements of an as-cast morphology of PDTSTPD subjected to thermal annealing. Plot of density against temperature showing that the onset of structural rearrangement occurred at approximately 107 °C. Images depicting 2 nm slices of simulation morphologies; individual molecules are colored separately, and side chains are not shown.

subjected to a heating protocol in which temperature was gradually increased while density was monitored. We observed that the density decreased slightly until approximately 110 °C (2). We attributed this initial thermal expansion to increased vibrations of the amorphous glass about metastable equilibrium positions. Above 110 °C there was a clear transition; the density started to increase with temperature. This behavior was evidently the result of chain segments escaping from metastable packing conformations and approaching an equilibrium state with better intermolecular packing. The density continued to increase with temperature until about 250 °C (3) where it peaked and the thermal expansion due to molecular vibrations dominated. Finally, at approximately 330 °C (4), an equilibrium melt was achieved, corresponding to the melting temperature measured using DSC for a structural analogue of the simulated polymer containing a branched side chain on the thienopyrrolodione (TPD) moiety.[51] When the melted system was subsequently quenched to room temperature (5), the density increased to a value substantially greater than that of the initial morphology.

CONCLUSION

The glass transition temperature is of paramount importance in determining the mechanical properties and thermal reliability of organic electronic devices. However, this property is not easy to measure using conventional techniques and often goes unreported. Facile techniques with broad applicability and which use simple equipment are necessary. This paper described a new method to determine the glass transition temperature of thin films of semicrystalline conjugated polymers. The technique uses quantitative analysis of the UV−vis absorption spectra of polymer films subjected to thermal annealing and requires only commonplace equipment. We tested the robustness of the technique through comparison with the literature for various well-characterized conjugated polymers and a BHJ composite (Figure 8). It is important to

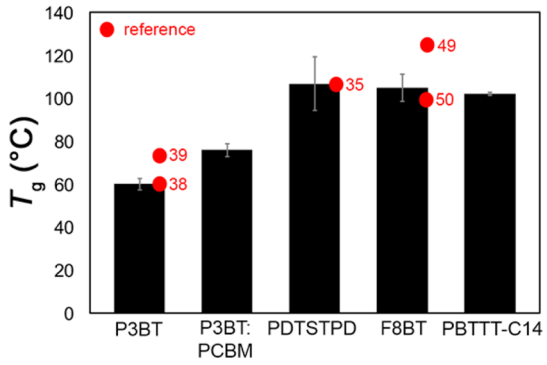

Figure 8. Summary of T_g measurements along with comparisons to the results of conventional techniques from the literature. Error bars are based on standard deviations between at least three separate films.

note that this technique works best for materials with a strong tendency to form ordered photophysical aggregates upon thermal annealing. For P3BT, an H-aggregate analysis of the absorption spectra revealed that the observed transition was dominated by an increase in the average conjugation length due to thermal relaxation of kinetically trapped dihedral states. MD simulations demonstrated in atomistic detail how a kinetically trapped morphology might rearrange due to the annealing of a solution-cast thin film. This technique should be of interest to organic materials chemists aiming to characterize the thermal properties of newly synthesized polymeric semiconductors and identify structure−property relationships required for molecular design.

EXPERIMENTAL METHODS

Materials. Poly(3-butylthiophene) (P3BT, M_n = 50−70 kDa, PDI = 2.1−3.0) was purchased from Rieke metals and used as received. Poly[2,5-bis(3-tetradecylthiophen-2-yl)-thieno[3,2-*b*]thiophene] (PBTTT-C14, M_n > 12 kDa, PDI = 1.8), poly(9,9-dioctylfluorene-*alt*-benzothiadiazole) (F8BT, M_n

DOI: 10.1021/acs.chemmater.7b00242
Chem. Mater. 2017, 29, 2646−2654

= 20−100 kDa), and poly[*N*-9′-heptadecanyl-2,7-carbazole-*alt*-5,5-(4′,7′-di-2-thienyl-2′,1′,3′-benzothiadiazole)] (PCDTBT, M_n = 20−100 kDa) were purchased from Lumtec and were used as received. Poly[(5,6-dihydro-5-octyl-4,6-dioxo-4*H*-thieno[3,4-*c*]pyrrole-1,3-diyl)[4,4-bis(2-ethylhexyl)-4*H*-silolo-[3,2-*b*:4,5-*b*′;]dithiophene-2,6-diyl]] (PDTSTPD, M_n = 7−35 kDa, PDI = 1.4−2.9), poly({4,8-bis[(2-ethylhexyl)oxy]benzo-[1,2-*b*:4,5-b′]dithiophene-2,6-diyl}{3-fluoro-2-[(2-ethylhexyl)-carbonyl]thieno[3,4-*q*]thiophenediyl}) (PTB7, M_n = 80−200 kDa, PDI < 3.0), poly[[2,3-bis(3-octyloxyphenyl)-5,8-quinoxalinediyl]-2,5-thiophenediyl] (TQ1, M_n = 12−45 kDa, PDI < 3.3), poly[2-methoxy-5-(2-ethylhexyloxy)-1,4-phenylenevinylene] (MEH-PPV, M_n = 40−70 kDa, PDI ≈ 6), [6.6]-phenyl C_{61} butyric acid methyl ester (PCBM), and 1,8-diiodooctane (DIO) were purchased from Sigma-Aldrich and used as received. Chloroform, acetone, and isopropyl alcohol (IPA) were obtained from Sigma-Aldrich and were used as received. Alconox was obtained from Alconox, Inc., and was used as received.

Preparation of Substrates. Glass slides, cut into squares (1 in. × 1 in.) with a diamond-tipped scribe, were used as substrates for the polymer thin films. The slides were thoroughly cleaned in an ultrasonic bath in the following sequence of 10 min steps: powdered Alconox detergent dissolved in deionized (DI) water, DI water only, acetone, and then IPA. After that, the slides were dried with compressed (house) air and then treated with plasma (30 W) for 5 min at a base pressure of 200 mTorr of air to remove residual organic debris and improve surface wettability.

Preparation of Films. Solutions of P3BT, P3BT:PCBM (0.8:1 by mass), PBTTT-C14, PDTSTPD, and F8BT in chloroform (10 mg mL^{-1}) were prepared and allowed to stir overnight. Prior to use, all solutions were slightly heated (∼15 s) with a heat gun to promote dissolution of the polymer. Next, the solutions were filtered with 0.20 μm PTFE filters, immediately after which they were spin-coated (Headway Research PWM32) onto the cleaned glass substrates at 2000 rpm (ramping at 1000 rpm s^{-1}) for 120 s. These conditions produced films of thicknesses ranging from 80 to 100 nm as determined by profilometry (Dektak 150 Surface Profiler). All films were dried under dynamic vacuum in the antechamber of a nitrogen-atmosphere glovebox (MBRAUN) for exactly 60 min to remove any residual chloroform.

Spectroscopic Characterization and Analysis. Once the freshly prepared thin films had dried under dynamic vacuum for an hour, their as-cast (UV−vis) spectra were acquired using an Agilent 8453 UV−vis spectrometer; the range of wavelengths measured was from 300 to 750 nm with a sampling increment of 1 nm (a pristine glass slide was used as a baseline for the absorption). The glass-supported films were then immediately heated for 5 min on the surface of a hot plate in a nitrogen-atmosphere glovebox, after which they were suspended in air and allowed to cool to room temperature (T_R, ∼25 °C) for 3 min prior to acquiring their "annealed" spectra. Starting at T_R, each film was annealed in various increments of temperature (5 °C, 10 °C, or 20 °C) depending on how far its nominal T_g was from T_R. The measurements were concluded once the annealing temperature sufficiently surpassed the nominal T_g of the polymer under investigation.

To correlate trends in aggregation and aggregate quality with annealing temperature, we have used the following model for H-aggregate absorption:

$$A \propto \sum_{m=0} \left(\frac{S^m}{m!}\right) \times \left(1 - \frac{We^{-s}}{2E_p} \sum_{n \neq m} \frac{S^n}{n!(n-m)}\right)^2 \times \exp\left(\frac{\left(E - E_0 - mE_p - \frac{1}{2}WS^m e^{-s}\right)^2}{2\sigma^2}\right) \quad (2)$$

where A is the absorption by an aggregate as a function of the photon energy E, W is the free exciton bandwidth, E_0 is the energy of the 0 → 0 vibronic transition, S is the Huang−Rhys factor (set to 1 for P3ATs), and E_p is the intermolecular vibration energy, which (in the case where S = 1) is the difference in energy between the vibrational levels in the excited state (set to 0.179 eV as determined by Raman spectroscopy). The terms m and n are the ground- and excited-state vibrational levels, and σ is the Gaussian line width.[32] The fitting parameters E_0, W, σ, and a scaling factor were found using MATLAB to perform a least-squares fit to the experimental absorption spectrum in the region of 1.93 to 2.25 eV.

Molecular Dynamics Simulations. All simulations and visualizations were performed with LAMMPS[55] and OVITO,[56] respectively. A detailed description of the atomistic model parametrization from electronic structure calculations as well as the simulation process for generating the as-cast morphology can be found elsewhere.[36,57] Briefly, 60 independent and isolated 12-mers were subjected to a simulated annealing process using Langevin dynamics (800 to 300 K over the course of 5 ns, NVT ensemble) in order to generate self-aggregated chain structures. These self-aggregated structures were randomly packed into a low-density simulation box (0.01 g cm^{-3}) and were subjected to NPT dynamics at 300 K and 1 atm using a Nosé−Hoover style thermostat (time constant = 100.0 fs) and barostat (time constant = 1000.0 fs) until the density converged (5 ns). Finally, the as-cast morphology was subjected to a thermal annealing protocol consisting of alternating runs between ramping the temperature (20 K ns^{-1}) and equilibrating (1 ns), while outputting the simulation trajectory and thermodynamic parameters.

■ ASSOCIATED CONTENT

Supporting Information

The Supporting Information is available free of charge on the ACS Publications website at DOI: 10.1021/acs.chemmater.7b00242.

Results of the technique as applied to predominantly amorphous polymers, heat transfer calculations, detailed description of data analysis, and effect of processing additive (PDF)

■ AUTHOR INFORMATION

Corresponding Author

*Darren Lipomi. E-mail: dlipomi@eng.ucsd.edu.

ORCID

Darren J. Lipomi: 0000-0002-5808-7765

Author Contributions

‡(S.E.R. and M.A.A.) These authors contributed equally.

Notes

The authors declare no competing financial interest.

DOI: 10.1021/acs.chemmater.7b00242
Chem. Mater. 2017, 29, 2646−2654

■ ACKNOWLEDGMENTS

This work was supported by the Air Force Office of Scientific Research (AFOSR) Grant Number FA9550-16-1-0220. Additional support was provided by the Hellman Fellowship awarded to D.J.L. and the Achievement Reward for College Scientists (ARCS) Fellowship awarded to S.E.R. Computational resources to support this work were provided by the Extreme Science and Engineering Discovery Environment (XSEDE) Program through the National Science Foundation Grant Number ACI-1053575.[58] Additionally, we would like to thank Professor Andrea Tao for use of the UV−vis spectrometer.

■ REFERENCES

(1) Müller, C. On the Glass Transition of Polymer Semiconductors and Its Impact on Polymer Solar Cell Stability. *Chem. Mater.* **2015**, *27*, 2740−2754.
(2) Savagatrup, S.; Printz, A. D.; O'Connor, T. F.; Zaretski, A. V.; Rodriquez, D.; Sawyer, E. J.; Rajan, K. M.; Acosta, R. I.; Root, S. E.; Lipomi, D. J. Mechanical Degradation and Stability of Organic Solar Cells: Molecular and Microstructural Determinants. *Energy Environ. Sci.* **2015**, *8*, 55−80.
(3) Mateker, W. R.; Mcgehee, M. D. Progress in Understanding Degradation Mechanisms and Improving Stability in Organic Photovoltaics. *Adv. Mater.* **2017**, *29*, 1603940.
(4) Strobl, G. *Physics of Polymers: Concepts for Understanding Their Structures and Behavior* **1997**, DOI: 10.1007/978-3-662-03488-0.
(5) Bennemann, C.; Donati, C.; Baschnagel, J.; Glotzer, S. C. Growing Range of Correlated Motion in a Polymer Melt on Cooling towards the Glass Transition. *Nature* **1999**, *399*, 246−249.
(6) Williams, M. L.; Landel, R. F.; Ferry, J. D. The Temperature Dependence of Relaxation Mechanisms in Amorphous Polymers and Other Glass-Forming Liquids. *J. Am. Chem. Soc.* **1955**, *77*, 3701−3707.
(7) O 'connor, T. F.; Rajan, K. M.; Printz, A. D.; Lipomi, D. J. Toward Organic Electronics with Properties Inspired by Biological Tissue. *J. Mater. Chem. B* **2015**, *3*, 4947−4952.
(8) Printz, A. D.; Lipomi, D. J. Competition between Deformability and Charge Transport in Semiconducting Polymers for Flexible and Stretchable Electronics. *Appl. Phys. Rev.* **2016**, *3*, 021302.
(9) Turi, E. *Thermal Characterization of Polymeric Materials*; Elsevier: 2012.
(10) Müller, C.; Andersson, L. M.; Garriga, M.; Campoy-quiles, M.; Peña-Rodríguez, O.; Inganäs, O. Determination of Thermal Transition Depth Profiles in Polymer Semiconductor Films with Ellipsometry. *Macromolecules* **2013**, *46*, 7325−7331.
(11) Schwartz, B. J. Conjugated Polymers as Molecular Materials: How Chain Conformation and Film Morphology Influence Energy Transfer and Interchain Interactions. *Annu. Rev. Phys. Chem.* **2003**, *54*, 141−172.
(12) Nikolka, M.; Nasrallah, I.; Rose, B.; Ravva, M. K.; Broch, K.; Harkin, D.; Charmet, J.; Hurhangee, M.; Brown, A.; Illig, S.; Too, P.; Jongman, J.; McCulloch, I.; Bredas, J.-L.; Sirringhaus, H.; Sadhanala, A. High Operational and Environmental Stability of High-Mobility Conjugated Polymer Field-Effect Transistors through the Use of Molecular Additives. *Nat. Mater.* **2016**, *16*, 356−362.
(13) Noriega, R.; Rivnay, J.; Vandewal, K.; Koch, F. P. V; Stingelin, N.; Smith, P.; Toney, M. F.; Salleo, A. A General Relationship between Disorder, Aggregation and Charge Transport in Conjugated Polymers. *Nat. Mater.* **2013**, *12*, 1038−1044.
(14) Holliday, S.; Donaghey, J. E.; McCulloch, I. Advances in Charge Carrier Mobilities of Semiconducting Polymers Used in Organic Transistors. *Chem. Mater.* **2014**, *26*, 647−663.
(15) Schroeder, B. C.; Chiu, Y.-C.; Gu, X.; Zhou, Y.; Xu, J.; Lopez, J.; Lu, C.; Toney, M. F.; Bao, Z. Non-Conjugated Flexible Linkers in Semiconducting Polymers: A Pathway to Improved Processability without Compromising Device Performance. *Adv. Electron. Mater.* **2016**, *2*, 1600104.
(16) Danley, R. L.; Reader, J. R.; Schaefer, J. W. Differential Scanning Calorimeter. U.S. Patent US5842788 A, 1998
(17) Rotter, G.; Ishida, H. Dynamic Mechanical Analysis of the Glass Transition: Curve Resolving Applied to Polymers. *Macromolecules* **1992**, *25*, 2170−2176.
(18) Kremer, F.; Andreas, S. *Broadband Dielectric Spectroscopy*; Springer: 2003.
(19) Beaucage, G.; Composto, R.; Stein, R. S. Ellipsometric Study of the Glass Transition and Thermal Expansion Coefficients of Thin Polymer Films. *J. Polym. Sci., Part B: Polym. Phys.* **1993**, *31*, 319−326.
(20) Lindqvist, C.; Wang, E.; Andersson, M. R.; Müller, C. Facile Monitoring of Fullerene Crystallization in Polymer Solar Cell Blends by UV-Vis Spectroscopy. *Macromol. Chem. Phys.* **2014**, *215*, 530−535.
(21) Tessarolo, M.; Guerrero, A.; Gedefaw, D.; Bolognesi, M.; Prosa, M.; Xu, X.; Mansour, M.; Wang, E.; Seri, M.; Andersson, M. R.; Muccini, M.; Garcia-Belmonte, G. Predicting Thermal Stability of Organic Solar Cells through an Easy and Fast Capacitance Measurement. *Sol. Energy Mater. Sol. Cells* **2015**, *141*, 240−247.
(22) Sung, M. J.; Luzio, A.; Park, W.-T.; Kim, R.; Gann, E.; Maddalena, F.; Pace, G.; Xu, Y.; Natali, D.; de Falco, C.; Dang, L.; McNeill, C. R.; Caironi, M.; Noh, Y.-Y.; Kim, Y.-H. High-Mobility Naphthalene Diimide and Selenophene-Vinylene-Selenophene-Based Conjugated Polymer: N-Channel Organic Field-Effect Transistors and Structure-Property Relationship. *Adv. Funct. Mater.* **2016**, *26*, 4984−4997.
(23) Lan, L.; Chen, Z.; Ying, L.; Huang, F.; Cao, Y. Acenaphtho[1,2-B]quinoxaline Diimides Derivative as a Potential Small Molecule Non-Fullerene Acceptor for Organic Solar Cells. *Org. Electron.* **2016**, *30*, 176−181.
(24) Patel, S. N.; Su, G. M.; Luo, C.; Wang, M.; Perez, L. A.; Fischer, D. A.; Prendergast, D.; Bazan, G. C.; Heeger, A. J.; Chabinyc, M. L.; Kramer, E. J. NEXAFS Spectroscopy Reveals the Molecular Orientation in Blade-Coated Pyridal[2,1,3]thiadiazole-Containing Conjugated Polymer Thin Films. *Macromolecules* **2015**, *48*, 6606−6616.
(25) Hufnagel, M.; Thelakkat, M. Simultaneous Morphological Stability and High Charge Carrier Mobilities in Donor−Acceptor Block Copolymer/PCBM Blends. *J. Polym. Sci., Part B: Polym. Phys.* **2016**, *54*, 1125−1136.
(26) Cho, E. C.; Chang-Jian, C. W.; Hsiao, Y. S.; Lee, K. C.; Huang, J. H. Influence of the Bridging Atom on the Electrochromic Performance of a Cyclopentadithiophene Polymer. *Sol. Energy Mater. Sol. Cells* **2016**, *150*, 43−50.
(27) Huth, H.; Minakov, A. A.; Serghei, A.; Kremer, F.; Schick, C. Differential AC-Chip Calorimeter for Glass Transition Measurements in Ultra Thin Polymeric Films. *Eur. Phys. J.: Spec. Top.* **2007**, *141*, 153−160.
(28) Keddie, J. L.; Jones, R. A. L.; Cory, R. A. Size-Dependent Depression of the Glass Transition Temperature in Polymer Films. *Epl* **1994**, *27*, 59−64.
(29) Printz, A. D.; Zaretski, A. V.; Savagatrup, S.; Chiang, A. S.-C.; Lipomi, D. J. Yield Point of Semiconducting Polymer Films on Stretchable Substrates Determined by Onset of Buckling. *ACS Appl. Mater. Interfaces* **2015**, *7*, 23257−23264.
(30) Printz, A. D.; Chiang, A. S. C.; Savagatrup, S.; Lipomi, D. J. Fatigue in Organic Semiconductors: Spectroscopic Evolution of Microstructure due to Cyclic Loading in poly(3-Heptylthiophene). *Synth. Met.* **2016**, *217*, 144−151.
(31) Kim, D. H.; Lee, B. L.; Moon, H.; Kang, H. M.; Jeong, E. J.; Park, J.-I.; Han, K. M.; Lee, S.; Yoo, B. W.; Koo, B. W.; Kim, J. Y.; Lee, W. H.; Cho, K.; Becerril, H. A.; Bao, Z. Liquid-Crystalline Semiconducting Copolymers with Intramolecular Donor-Acceptor Building Blocks for High-Stability Polymer Transistors. *J. Am. Chem. Soc.* **2009**, *131*, 6124−6132.
(32) Clark, J.; Chang, J. F.; Spano, F. C.; Friend, R. H.; Silva, C. Determining Exciton Bandwidth and Film Microstructure in Polythiophene Films Using Linear Absorption Spectroscopy. *Appl. Phys. Lett.* **2009**, *94*, 163306.

DOI: 10.1021/acs.chemmater.7b00242
Chem. Mater. 2017, 29, 2646−2654

(33) Pingel, P.; Zen, A.; Abellón, R. D.; Grozema, F. C.; Siebbeles, L. D. A.; Neher, D. Temperature-Resolved Local and Macroscopic Charge Carrier Transport in Thin P3HT Layers. *Adv. Funct. Mater.* **2010**, *20*, 2286−2295.
(34) Chu, T. Y.; Lu, J.; Beaupré, S.; Zhang, Y.; Pouliot, J. R.; Zhou, J.; Najari, A.; Leclerc, M.; Tao, Y. Effects of the Molecular Weight and the Side-Chain Length on the Photovoltaic Performance of Dithienosilole/thienopyrrolodione Copolymers. *Adv. Funct. Mater.* **2012**, *22*, 2345−2351.
(35) Chu, T.-Y.; Lu, J.; Beaupre, S.; Zhang, Y.; Pouliot, J.-R.; Wakim, S.; Zhou, J.; Leclerc, M.; Li, Z.; Ding, J.; Tao, Y. Bulk Heterojunction Solar Cells Using Thieno[3,4-C]pyrrole-4,6-Dione and Dithieno[3,2-b:2′,3′-d]silole Copolymer with a Power Conversion Efficiency of 7.3%. *J. Am. Chem. Soc.* **2011**, *133*, 4250−4253.
(36) Root, S. E.; Jackson, N.; Savagatrup, S.; Arya, G.; Lipomi, D. J. Modelling the Morphology and Thermomechanical Behaviour of Low-Bandgap Conjugated Polymers and Bulk Heterojunction Films. *Energy Environ. Sci.* **2017**, *10*, 558−569.
(37) Cho, S.; Seo, J. H.; Park, S. H.; Beaupré, S.; Leclerc, M.; Heeger, A. J. A Thermally Stable Semiconducting Polymer. *Adv. Mater.* **2010**, *22*, 1253−1257.
(38) Chen, S.; Ni, J. Structure/properties of Conjugated Conductive Polymers. 1. Neutral Poly (3-Alkythiophene) S. *Macromolecules* **1992**, *25*, 6081−6089.
(39) Yazawa, K.; Inoue, Y.; Yamamoto, T.; Asakawa, N. Twist Glass Transition in Regioregulated poly(3-Alkylthiophene). *Phys. Rev. B: Condens. Matter Mater. Phys.* **2006**, *74*, 094204.
(40) Spano, F. C. Modeling Disorder in Polymer Aggregates: The Optical Spectroscopy of Regioregular poly(3-Hexylthiophene) Thin Films. *J. Chem. Phys.* **2005**, *122*, 234701.
(41) Spano, F. C. The Spectral Signatures of Frenkel Polarons in H- And J-Aggregates. *Acc. Chem. Res.* **2010**, *43*, 429−439.
(42) Awartani, O.; Lemanski, B. I.; Ro, H. W.; Richter, L. J.; De Longchamp, D. M.; O'Connor, B. T. Correlating Stiffness, Ductility, and Morphology of polymer:Fullerene Films for Solar Cell Applications. *Adv. Energy Mater.* **2013**, *3*, 399−406.
(43) Guilbert, A. A. Y.; Zbiri, M.; Jenart, M. V. C.; Nielsen, C. B.; Nelson, J. New Insights into the Molecular Dynamics of P3HT:PCBM Bulk Heterojunction: A Time-of-Flight Quasi-Elastic Neutron Scattering Study. *J. Phys. Chem. Lett.* **2016**, *7*, 2252−2257.
(44) Root, S. E.; Savagatrup, S.; Pais, C. J.; Arya, G.; Lipomi, D. J. Predicting the Mechanical Properties of Organic Semiconductors Using Coarse-Grained Molecular Dynamics Simulations. *Macromolecules* **2016**, *49*, 2886−2894.
(45) McCulloch, I.; Heeney, M.; Bailey, C.; Genevicius, K.; Macdonald, I.; Shkunov, M.; Sparrowe, D.; Tierney, S.; Wagner, R.; Zhang, W.; Chabinyc, M. L.; Kline, R. J.; McGehee, M. D.; Toney, M. F. Liquid-Crystalline Semiconducting Polymers with High Charge-Carrier Mobility. *Nat. Mater.* **2006**, *5*, 328−333.
(46) DeLongchamp, D. M.; Kline, R. J.; Jung, Y.; Lin, E. K.; Fischer, D. A.; Gundlach, D. J.; Cotts, S. K.; Moad, A. J.; Richter, L. J.; Toney, M. F.; Heeney, M.; McCulloch, I. Molecular Basis of Mesophase Ordering in a Thiophene-Based Copolymer. *Macromolecules* **2008**, *41*, 5709−5715.
(47) Miller, N. C.; Gysel, R.; Miller, C. E.; Verploegen, E.; Beiley, Z.; Heeney, M.; McCulloch, I.; Bao, Z.; Toney, M. F.; McGehee, M. D. The Phase Behavior of a Polymer-Fullerene Bulk Heterojunction System That Contains Bimolecular Crystals. *J. Polym. Sci., Part B: Polym. Phys.* **2011**, *49*, 499−503.
(48) Kim, Y.; Cook, S.; Choulis, S. a.; Nelson, J.; Durrant, J. R.; Bradley, D. D. C. Organic Photovoltaic Devices Based on Blends of Regioregular Poly(3-Hexylthiophene) and Poly(9,9-Dioctylfluorene-Co -Benzothiadiazole). *Chem. Mater.* **2004**, *16*, 4812−4818.
(49) Banach, M. J.; Friend, R. H.; Sirringhaus, H. Influence of the Molecular Weight on the Thermotropic Alignment of Thin Liquid Crystalline Polyfluorene Copolymer Films. *Macromolecules* **2003**, *36*, 2838−2844.
(50) Campoy-Quiles, M.; Sims, M.; Etchegoin, P. G.; Bradley, D. D. C. Thickness-Dependent Thermal Transition Temperatures in Thin Conjugated Polymer Films. *Macromolecules* **2006**, *39*, 7673−7680.
(51) Yuan, M. C.; Chou, Y. J.; Chen, C. M.; Hsu, C. L.; Wei, K. H. A Crystalline Low-Bandgap Polymer Comprising Dithienosilole and thieno[3,4-C]pyrrole-4,6-Dione Units for Bulk Heterojunction Solar Cells. *Polymer* **2011**, *52*, 2792−2798.
(52) Bergqvist, J.; Lindqvist, C.; Bäcke, O.; Ma, Z.; Tang, Z.; Tress, W.; Gustafsson, S.; Wang, E.; Olsson, E.; Andersson, M. R.; Inganäs, O.; Müller, C. Sub-Glass Transition Annealing Enhances Polymer Solar Cell Performance. *J. Mater. Chem. A* **2014**, *2*, 6146−6152.
(53) Root, S. E.; Jackson, N.; Savagatrup, S.; Arya, G.; Lipomi, D. J. Modelling the Morphology and Thermomechanical Behaviour of Low-Bandgap Conjugated Polymers and Bulk Heterojunction Films. *Energy Environ. Sci.* **2017**, *10*, 558−569.
(54) Fauvell, T. J.; Zheng, T.; Jackson, N. E.; Ratner, M. A.; Yu, L.; Chen, L. X. The Photophysical and Morphological Implications of Single-Strand Conjugated Polymer Folding in Solution. *Chem. Mater.* **2016**, *28*, 2814−2822.
(55) Plimpton, S. Fast Parallel Algorithms for Short-Range Molecular Dynamics. *J. Comput. Phys.* **1995**, *117*, 1−19.
(56) Stukowski, A. Visualization and Analysis of Atomistic Simulation Data with OVITO−the Open Visualization Tool. *Modell. Simul. Mater. Sci. Eng.* **2010**, *18*, 015012.
(57) Jackson, N. E.; Kohlstedt, K. L.; Savoie, B. M.; Olvera de la Cruz, M.; Schatz, G. C.; Chen, L. X.; Ratner, M. a. Conformational Order in Aggregates of Conjugated Polymers. *J. Am. Chem. Soc.* **2015**, *137*, 6254−6262.
(58) Towns, J.; Cockerill, T.; Foster, I.; Gaither, K.; Dahan, M.; Grimshaw, A.; Hazlewood, V.; Lathrop, S.; Lifka, D.; Peterson, G. D.; et al. XSEDE: Accelerating Scientific Discovery. *Comput. Sci. Eng.* **2014**, *16*, 62−74.

DOI: 10.1021/acs.chemmater.7b00242
Chem. Mater. 2017, 29, 2646−2654